Well-Defined Block Copolymers with Triphenylamine and Isocyanate Moieties Synthesized via Living Anionic Polymerization for Polymer-Based Resistive Memory Applications: Effect of Morphological Structures on Nonvolatile Memory Performances

Beom-Goo Kang,[†,§] Jingon Jang,[‡] Younggul Song,[‡] Myung-Jin Kim,[†] Takhee Lee,*[‡] and Jae-Suk Lee*[†]

[†]School of Materials Science and Engineering, Gwangju Institute of Science and Technology (GIST), 123 Cheomdangwagi-ro, Buk-gu, Gwangju 500-712, Korea

[‡]Department of Physics and Astronomy, and Institute of Applied Physics, Seoul National University, Seoul 151-747, Korea

[§]Department of Chemistry, University of Tennessee, Knoxville, Tennessee 37996, United States

Ⓢ *Supporting Information*

ABSTRACT: The anionic block copolymerization of 4,4′-vinyl-phenyl-*N,N*-bis(4-*tert*-butylphenyl)benzenamine (**A**) with *n*-hexyl isocyanate (**B**) was performed using potassium naphthalenide (K-Naph) in THF at −78 and −98 °C in the presence of sodium tetraphenylborate (NaBPh$_4$) to afford the well-defined block copolymers for investigating the effect of morphological structures on electrical memory performances. The well-defined functional block copolymers (P**BAB**) with different block ratios had predictable molecular weights (M_n = 17 700−79 100 g/mol) and narrow molecular weight distributions (M_w/M_n = 1.14−1.19). It was observed from transmission electron microscopy (TEM) that the block copolymers showed different morphological structures depending on block ratios. Although all memory devices fabricated from the resulting block copolymers with different block compositions equally exhibited nonvolatile resistive switching characteristics, which are governed by the trap-controlled space-charge-limited current (SCLC) conduction mechanism and filament formation, it was found that electrical memory performances of each device varied depending on morphological structures of the block copolymer films.
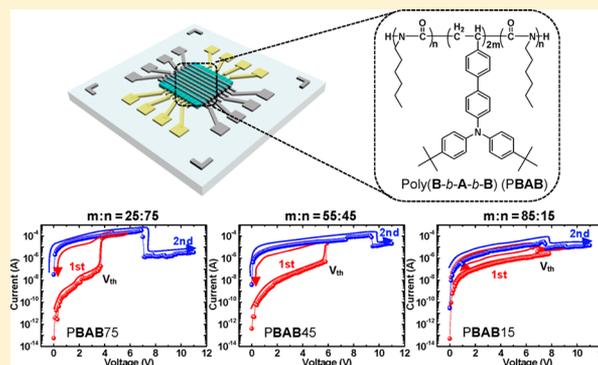
■ INTRODUCTION

The side-chain polymers with pendent triphenylamine are known as suitable materials for hole-transporting layers in polymer light-emitting diodes (PLEDs) due to their good hole-transporting capacity and high thermal stability.[1−5] Although a variety of polymerization methods were used to prepare the polymers with pendent triphenylamine, the well-defined polymers with predictable molecular weights (M_n) and narrow molecular weight distributions (M_w/M_n) could be synthesized by anionic polymerization.[6−8] In particular, our group reported that the introduction of *tert*-butyl protecting group to the triphenylamine prevented the side reactions occurring in the anionic polymerization of 4,4′-vinylphenyltriphenylamine. The living anionic polymerization of 4,4′-vinylphenyl-*N,N*-bis(4-*tert*-butylphenyl)benzenamine (**A**) has been successfully carried out using K-Naph in THF at −78 °C for 0.5 h.[8]

From the synthetic point of view, living character of **A** could make it possible to create well-defined functional block copolymers containing **A** block in anionic systems, and the resulting block copolymers could be used for applications in polymer-based electronic devices.[9−11] For example, thermally

cross-linkable block copolymer consisting of a triphenylamine group as the hole transporting moiety and an ethynyl group as the thermal cross-linker, poly(4-ethynylstyrene)-*b*-poly(**A**)-*b*-poly(4-ethynylstyrene), has been synthesized by living anionic polymerization and deprotection process and used as an effective alternative hole-transporting layer to PEDOT:PSS in PLEDs.[9] The functional block copolymer with pendent donor−acceptor, poly(2-(2-(4-vinylphenyl)ethynyl)pyridine)-*b*-poly-(**A**)-*b*-poly(2-(2-(4-vinylphenyl)ethynyl)pyridine), has been also synthesized using K-Naph in THF at −78 °C without any additives and used as an active layer in polymer-based memory devices. The memory devices fabricated with the resulting block copolymer showed high performances in terms of nonvolatile memory characteristics.[11] Accordingly, such successful synthesis of the well-defined functional block copolymers mentioned above allowed us to further try to synthesize various kinds of block copolymers containing **A**

Table 1. Block Copolymerization of A with B Using K-Naph in THF in the Presence of NaBPh$_4$

| | | monomer | | | block copolymer (homopolymer) | | | |
| | | | | | $M_n \times 10^{-3}$ | | | |
sample	K-Naph (mmol)	1st, mmol	2nd, mmol	NaBPh$_4$ (mmol)	calcd[a]	obsd[b]	M_w/M_n[c]	$f_{\text{poly(B)}}$[d]
PBAB75	0.0497	A, 0.581	B, 1.98	0.558	20.8 (10.7)	17.7 (9.6)	1.19 (1.10)	0.75
PBAB45	0.0518	A, 1.22	B, 0.885	0.632	26.1 (21.7)	23.9 (19.4)	1.16 (1.10)	0.45
PBAB15	0.0270	A, 1.96	B, 0.458	0.641	71.0 (66.7)	79.1 (75.1)	1.14 (1.16)	0.15

[a]M_n(calcd) = (molecular weight of monomer) × [monomer] × 2/[initiator]. [b]M_n of the block copolymer was determined by using M_n of the homopolymer and the molar ratio of each block estimated by ^{1}H NMR. [c]M_w/M_n was determined by using SEC calibration with polystyrene standards in a THF solution containing 2% triethylamine as the eluent at 40 °C. [d]Determined by ^{1}H NMR.

block, which might be used as appropriate materials for polymer-based electronic devices applications.

Very recently, significant effects of the morphological structures of the block copolymers on the electrical memory characteristics have been reported.[12−14] In these reports, it was demonstrated that various phase-separated nanostructures of the well-defined block copolymers formed by thermal or solvent annealing directly related to the memory characteristics. A memory mode could be converted to the other modes, such as nonvolatile, volatile, and dielectric characteristics, by changing morphological structures. However, a few researches on effect of the block copolymer morphologies on the electrical memory behaviors have been conducted to date, and thus structural and electrical characterizations of block copolymer-based memory devices have not yet been fully understood. Therefore, it is important not only to establish the relationship between morphological structures and electrical memory behaviors but also to synthesize diverse kinds of well-controlled block copolymers in order to further develop the performances of block copolymer-based memory devices. For the purpose of investigating the relationship, the anionic polymerization technique that has been well-known to prepare the block copolymers with precise molecular structures is necessarily required because the effect of the morphological structures on electrical memory characteristics can be exactly investigated from the well-defined block copolymers.[15−19]

In general, vinyl monomers cannot be polymerized by the living polyisocyanate because reactivity of amidate anions of polyisocyanate is relatively very weak. Thus, block copolymerization has to be carried out by sequential addition of vinyl monomer as the first monomer and isocyanate as the second monomer to precisely synthesize block copolymers containing isocyanate. Very few studies on the block copolymerization of isocyanate with vinyl monomers have been performed due to the challenge of controlling the polymerization of isocyanate. In our group, we have established the optimum conditions for successful block copolymerization of styrene and 2-vinylpyridine with *n*-hexyl isocyanate (**B**).[20,21] The well-controlled rod−coil−rod triblock copolymer, poly(**B**)-*b*-polystyrene-*b*-poly(**B**), and coil−rod diblock copolymer, poly(2-vinylpyridine)-*b*-poly(**B**), were successfully prepared in the presence of sodium tetraphenylborate (NaBPh$_4$), which prevents backbiting reactions (formation of trimers) during the polymerization of **B**.

On the basis of these researches, we chose **B** as a comonomer, in this study, to synthesize the well-defined poly(**B**-*b*-**A**-*b*-**B**) (**PBAB**) via living anionic polymerization. The block copolymers containing **A** block as a conducting component and **B** block as an insulating component were quantitatively produced using K-Naph in the presence of NaBPh$_4$ without any side reactions. Since the well-defined

block copolymers can form a variety of morphological structures depending on the block compositions, PBABs with different block ratios (**A** block:**B** block (mol %) = 25:75, 55:45, and 85:15) were precisely prepared via living anionic polymerization in order to investigate the effect of the morphological structures of the resulting block copolymers on electrical memory performances.

■ EXPERIMENTAL SECTION

Materials. 4,4′-Vinylphenyl-*N*,*N*-bis(4-*tert*-butylphenyl)-benzenamine (**A**) and K-Naph were prepared according to papers previously reported.[6,22] *n*-Hexyl isocyanate (**B**, Aldrich, 97%) was dried overnight over calcium hydride (CaH$_2$) and distilled under reduced pressure. **B** was finally distilled from CaH$_2$ on a vacuum line into ampules equipped with break-seals. Sodium tetraphenylborate (NaBPh$_4$, Aldrich, 99.5%) was dried under high vacuum with heating for 3 days. All materials were diluted with THF and divided into ampules equipped with break-seals. The ampules were kept at −30 °C prior to polymerization.

Measurements. The polymers were characterized by size exclusion chromatography (SEC, Waters M77251, M510). The molecular weight distributions of the polymers were determined using SEC calibration with polystyrene standards (American Polymer Standards Corp.) in a THF solution containing 2% triethylamine as the eluent at 40 °C. ^{1}H NMR spectra were obtained using CDCl$_3$ as a solvent at 25 °C (JEOL JNM-ECX400). The chemical shifts are in reference to tetramethylsilane (TMS) at 0 ppm. The morphologies of the block copolymers were characterized with a field emission transmission electron microscope (FE-TEM, JEOL JEM-2100F).

Block Copolymerization. The first-stage polymerization of **A** was carried out with K-Naph in THF at −78 °C for 0.5 h in an all-glass apparatus equipped with break-seals under high vacuum. After a portion of the living poly(**A**) was sampled to characterize, NaBPh$_4$ was added into the living poly(**A**) solution at −98 °C. **B** was then added to the solution, and the reaction was continued at −98 °C for 0.5 h. The reaction solutions, terminated with methanol, were poured into a large amount of methanol to obtain both poly(**A**) and **PBAB**. The detailed synthetic procedure is explained in the Supporting Information (Figure S1). The yield of block copolymer was quantitative. The resulting block copolymer was characterized by SEC and ^{1}H NMR. **PBAB** (M_n(obsd) = 17 700 g/mol, M_w/M_n = 1.19 (Table 1, **PBAB**75)). ^{1}H NMR (400 MHz, CDCl$_3$): δ = 0.88 (CH$_3$ in hexyl group of **B** block), 1.10−1.87 ((CH$_2$)$_4$ in hexyl group of **B** block, CH$_2$−CH and *tert*-butyl group of **A** block), 3.65 (−CH$_2$−N in hexyl group of **B** block), 6.35−7.58 (phenyl group of **A** block).

Fabrication and Characterization of Memory Device. The fabrication process of our organic memory devices with a PBAB active layer is shown in Figure 4. ITO/PBAB/Al devices with an 8 × 8 cross-bar array structure were fabricated. First, a bare glass substrate was cleaned by a standard solvent cleaning process (using acetone, isopropyl alcohol, and deionized water in an ultrasonic bath for 10 min, respectively) and dried with N$_2$ gas. The bottom ITO electrodes were deposited and subsequently patterned with eight lines by conventional photolithography and wet etching process. The PBAB dissolved in toluene (1.0 wt %) was spin-coated onto the bottom ITO

Scheme 1. Synthetic Route for PBAB

Poly(**B**-*b*-**A**-*b*-**B**) (PBAB)
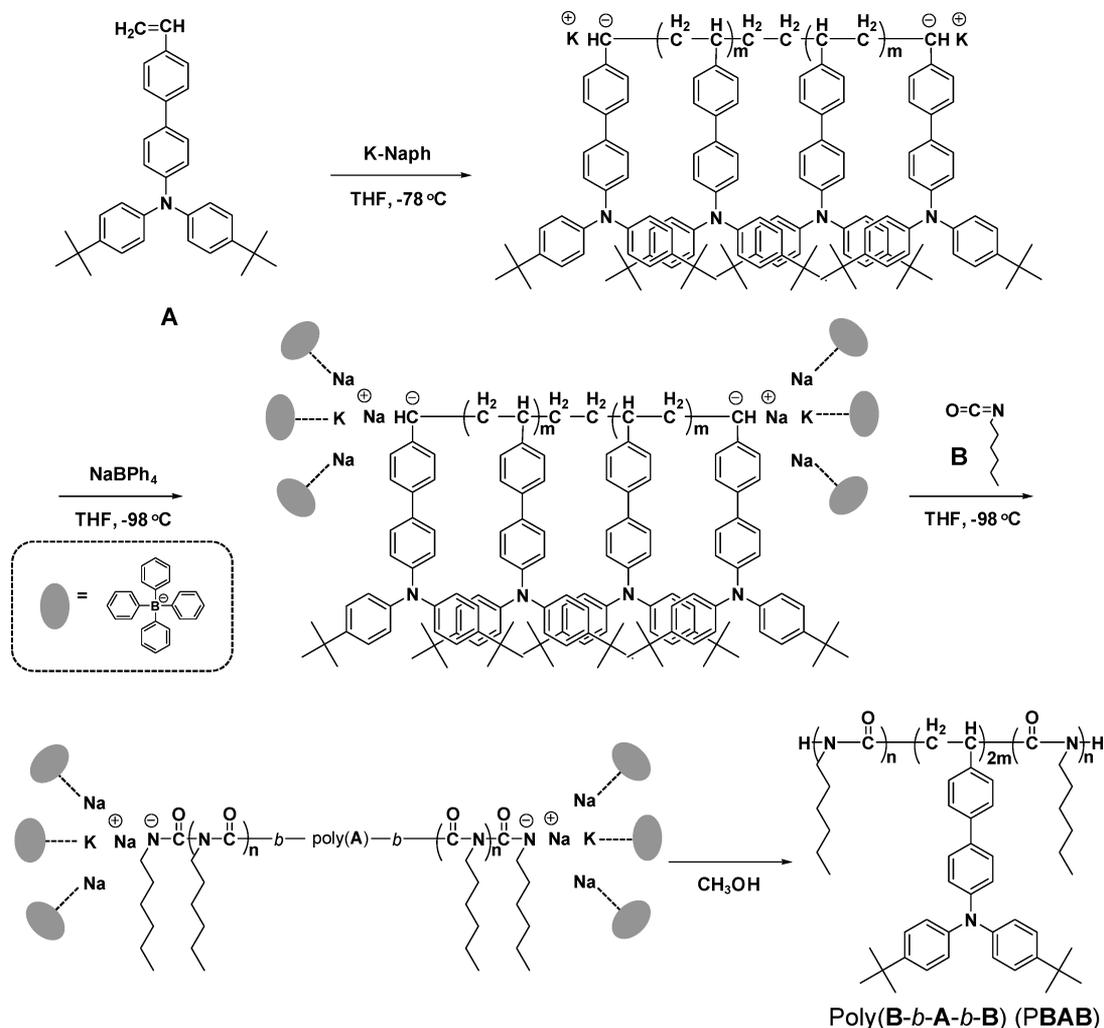
electrodes at 2000 rpm for 35 s. The coated film was soft-baked on a hot plate at 60 °C for 5 min enough to dry the toluene solvent from organic active layer. Then, the film on the contact pads of bottom ITO electrodes was removed using methanol for the electrical measurements, followed by hard-baking on the hot plate at 110 °C for 60 min. Finally, the top Al electrodes were deposited by a thermal evaporator using a shadow mask with eight lines. To electrically characterize the fabricated memory devices, we performed current–voltage (*I*–*V*) measurements with a Keithley 4200 SCS semiconductor analyzing system in a N$_2$-filled glovebox system at room temperature.

■ RESULTS AND DISCUSSION

From the synthetic viewpoint, the living character of **A**, proved by the anionic polymerization with K-Naph in THF at −78 °C, can offer an opportunity to prepare a variety of well-defined block copolymers containing **A** block through the sequential block copolymerization with various functional monomers.[6,9−11] This finding allowed us to synthesize the well-defined functional block copolymers consisting of conducting and insulating block. Here, **A** and **B** were selected as monomers for conducting and insulating block, respectively. Based on our previous investigations on precise synthesis of poly(**B**)-*b*-polystyrene-*b*-poly(**B**) and poly(2-vinylpyridine)-*b*-poly-(**B**),[20,21] the block copolymerization was performed by sequential addition of **A** as the first monomer and **B** as the second monomer using K-Naph as an initiator in THF at −78

and −98 °C in the presence of NaBPh$_4$, as shown in Scheme 1. First, **A** was polymerized at −78 °C, and then excess NaBPh$_4$ was subsequently added at −98 °C to exchange countercation from K$^+$ to Na$^+$ for the living anionic polymerization of **B**. When **B** was added into the living poly(**A**) solution at −98 °C, the color of polymerization solution immediately changed from deep violet to pale yellow, indicating that amidate anions are successfully formed. This solution color distinctly retained until polymerization was terminated with methanol.

From the ^{1}H NMR spectra of **A**, **B**, and the resulting **PBAB**, it was found that the block copolymerization proceeded exclusively. As shown in Figure 1, the broad characteristic peaks of *tert*-butyl, phenyl, and hexyl groups were observed after polymerization, whereas the peaks of vinyl group of monomer **A** completely disappeared. Table 1 suggests that the block copolymers were precisely synthesized. The polymers possessed predictable M_n (17 700−79 100 g/mol) and narrow M_w/M_n (1.14−1.19). For instance, the polymerization proceeded quantitatively with K-Naph in THF at −78 and −98 °C for 1 h in the presence of NaBPh$_4$ (Table 1, PBAB75). The observed M_n (17 700 g/mol) agreed well with the expected one (20 800 g/mol). Furthermore, the SEC curve of the resulting block copolymer was narrow (M_w/M_n = 1.19) and shifted from the starting poly(**A**) toward the higher M_n region, as shown in Figure 2 (SEC curves of PBAB45 and PBAB15 are
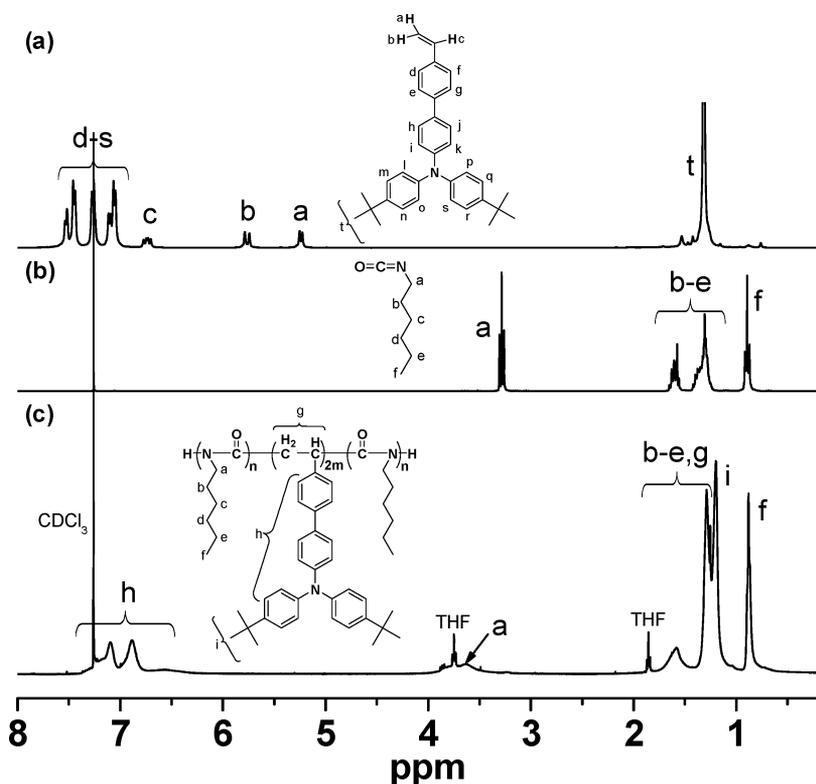
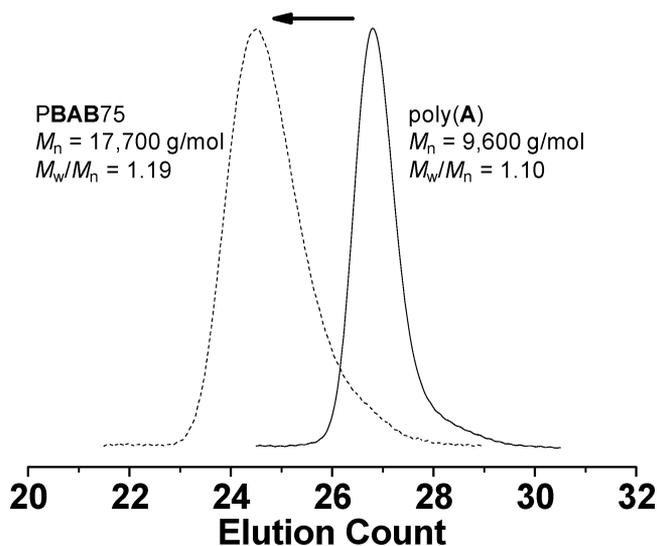**Figure 1.** ^{1}H NMR spectra of (a) **A**, (b) **B**, and (c) **PBAB** in CDCl$_3$.

Figure 2. SEC curves of poly(**A**) and **PBAB**75.

shown in Figure S2 of the Supporting Information.). From these results of the block copolymerization of **A** with **B**, it is believed that the propagating chain-end of poly(**A**) can polymerize **B** without unwanted side reactions under the polymerization conditions employed here, indicating that the use of K$^+$ as the countercation for the polymerization of **A** and Na$^+$ (NaBPh$_4$) for the polymerization of **B** results in the formation of the well-controlled novel triblock copolymers.

The previous studies on relationship between film morphologies and electrical properties of block copolymer-based nonvolatile memory device demonstrated that the devices based on block copolymer system showing well-ordered microphase-separated structures exhibit nonvolatile

resistive switching characteristics with excellent memory performances.[9,14] On the basis of these researches, we attempted to observe well-ordered microphase-separated structures from three **PBAB** with different block ratios. From here, the block copolymers with block ratios (mol %) of **A** block:**B** block = 25:75, 55:45, and 85:15 are simply denoted as **PBAB**75, **PBAB**45, and **PBAB**15, respectively. The polymer solutions in toluene were drop-casted onto the carbon-coated copper grid and baked at 110 °C for 60 min. The iodine (I$_2$) was subsequently used for 11 h to stain the samples. As shown in Figure 3, the well-ordered microphase-separated morphological structures of **PBAB**75 were only observed from TEM; in contrast, **PBAB**45 and **PBAB**15 showed poorly ordered structures. In TEM images, **A** and **B** block were shown as white and black, respectively, because **B** block was stained by I$_2$ vapor. All the resulting block copolymers were soluble in THF, benzene, toluene, and chlorobenzene. In particular, the polymer solutions dissolved in toluene were well spin-coated on the substrate. From these characterizations, the block copolymers that show different morphological behaviors depending on block ratios and good film-forming properties could be potential materials for investigating the effect of the morphological structures on electrical memory performances.

The inset of Figure 5a shows the schematic illustration of our array-type organic memory devices consisting of ITO/**PBAB**/Al layers. Positive voltage was applied to Al top electrodes while ITO bottom electrodes were grounded. Figure 5a−c shows representative semilogarithmic $I-V$ characteristics of the memory devices with **PBAB**75, **PBAB**45, and **PBAB**15, respectively. It is shown that all of these three $I-V$ curves precisely exhibit typical unipolar resistive memory switching in which writing and erasing process are available in the same voltage polarity.[23] The unipolar switching is particularly important for practical memory applications because applica-
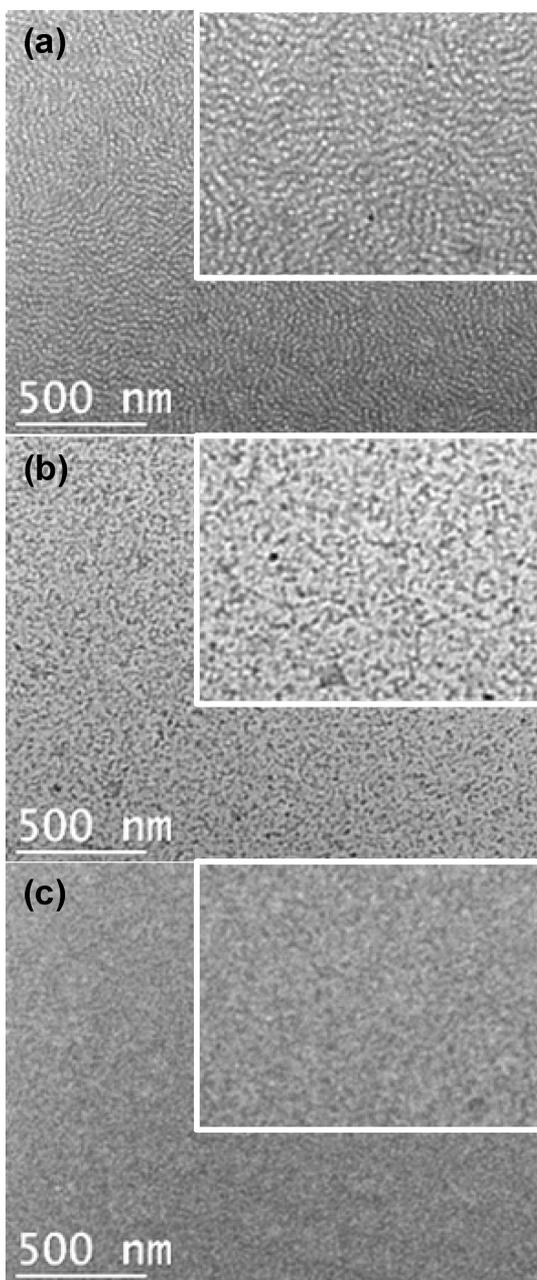
Figure 3. TEM images of (a) PBAB75, (b) PBAB45, and (c) PBAB15.

tion of device structure type of one diode and one resistor (1D-1R) which can prevent selected cell from cross-talk interruption is only available in unipolar type resistive memory.[24] In the case of PBAB75 memory devices (Figure 5a), the current of the devices kept low in the low voltage region, indicating a high resistance state (OFF state), and then gradually increased as the applied voltage further increased. The current then rapidly increased when the voltage reached ~4 V, switching the memory devices to a low resistance state (ON state). During the recovery from 6 to 0 V in the first dual sweep mode, the ON state was stably maintained. After that, when the second single sweeping voltage was applied to devices from 0 to 11 V, the ON current state still remained in the low voltage region, representing the nonvolatile memory effect. The ON current was suddenly decreased when the voltage reached ~7 V, showing negative differential resistance (NDR) in the high
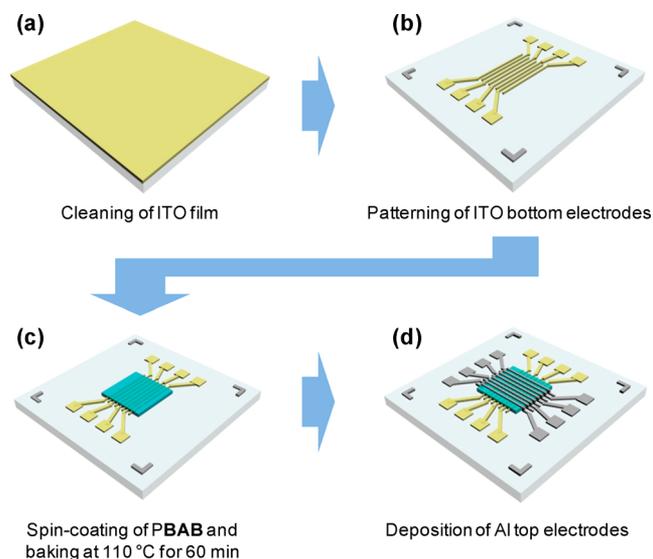

Figure 4. Schematic illustration of the fabrication processes of ITO/PBAB/Al device with an 8 × 8 array structure.

voltage region (reset process). This means that the device has rewritable switching characteristics, which can open a way to more practical memory applications compared to write-once read-many times (WORM) memory devices. Similarly, PBAB45 (Figure 5b) and PBAB15 (Figure 5c) memory devices also showed the unipolar resistive memory switching; however, the larger threshold voltages were needed for the cases of PBAB45 (~5.5 V) and PBAB15 (~6 V) compared to PBAB75 (~4 V). In addition, it was found that the ON current showed the decreasing tendency with decreasing mole fraction of B block, meaning that PBAB75 exhibited the highest ON/OFF ratio among three kinds of devices.

$I-V$ curves were analyzed by using a double-log $I-V$ plot in order to figure out the conduction mechanisms of PBAB-based memory devices. A double-log $I-V$ plot of PBAB75 memory devices is representatively shown in Figure 5d. (The double-log $I-V$ plots of PBAB45 and PBAB15 memory devices are shown in Figure S3 of the Supporting Information.) A transition behavior in charge conduction was observed in the OFF state. In the low voltage region (0 to ~4 V) of the OFF state, the current was linearly proportional to the applied voltage, indicating general ohmic conduction behavior ($I \propto V$); in contrast, the current increased nonlinearly in the high voltage region of the OFF state ($I \propto V^8$). The value of $I-V$ slope implied that the charge transport in the OFF state can be explained by trap-controlled space-charge-limited current (SCLC) model.[25−28] As shown in Figure 6, poly(**A**) and poly(**B**) clearly exhibited high and low current levels, respectively, without any switching behaviors. These electrical properties of poly(**A**) and poly(**B**) strongly indicate that the resistive memory switching of the ITO/PBAB/Al devices is likely due to the presence of the PBAB block copolymer interlayer. From the $I-V$ characteristics of poly(**A**) and poly(**B**), it can be suggested that the conducting **A** block in the block copolymers might act as charge-trapping sites. As the voltage was applied to the block copolymer interlayer, a large number of charge carriers were injected from the Al electrodes. These charge carriers were trapped in the **A** block segment, and the OFF state was maintained until all traps are filled. After the threshold voltage, the current state abruptly switched to the
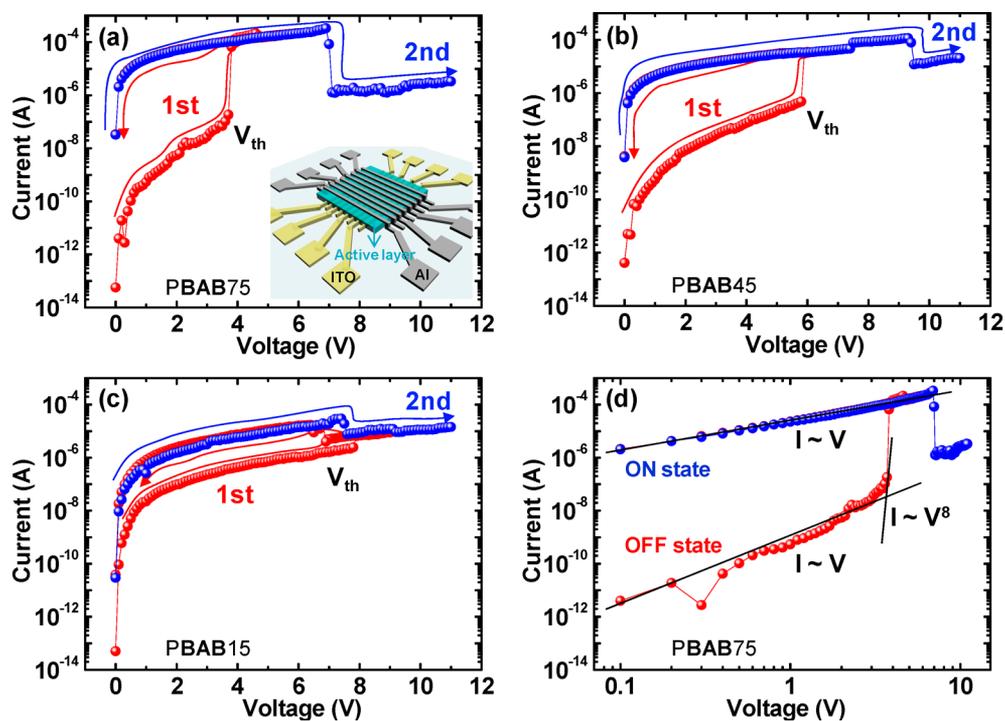
Figure 5. Current−voltage (*I*−*V*) switching characteristics of (a) P**BAB**75, (b) P**BAB**45, and (c) P**BAB**15. (d) A double-log *I*−*V* plot analysis of P**BAB**75. Inset of (a): schematic illustration of 8 × 8 array-type memory device consisting of ITO/P**BAB**/Al layers.
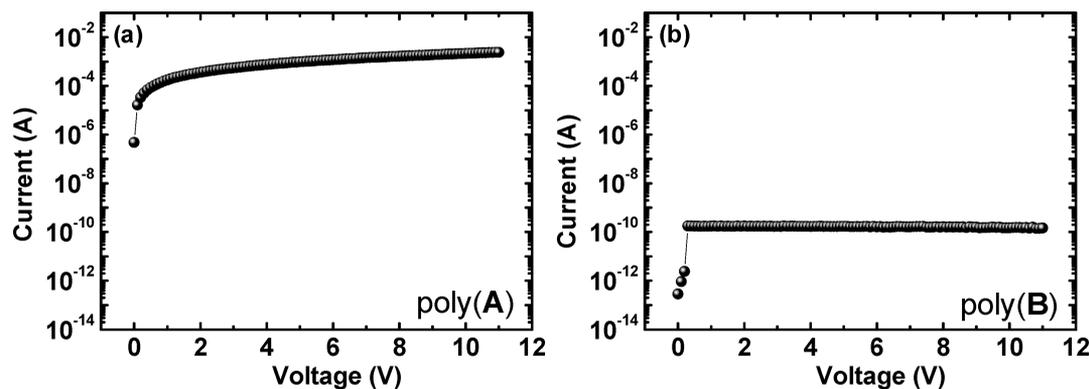

Figure 6. *I*−*V* characteristics of (a) poly(**A**) and (b) poly(**B**).

ON state. Therefore, it is shown in Figure 5d that the conduction behavior changed from SCLC transport state to the ohmic state, indicating that the ON current was related to the filamentary conduction.[29−31] For the possible mechanism for our memory devices, we now believe that conductive paths mainly consisting of triphenylamine units of **A** block might be formed or ruptured by an electrical field.[9,14]

In array-type memory devices, it is essential to evaluate the device parameters of the operating cells statistically. Figure 7 shows the cumulative probability of the switching current and statistical distributions of the threshold voltages in each P**BAB**-based memory device. Here, the OFF (ON) current values indicate the measured data at a read voltage of 0.3 V in the forward (backward) direction of the first dual sweep hysteresis and threshold voltages mean the setting voltage from OFF resistive state to ON resistive state. For the case of P**BAB**75 memory devices (Figure 7a), the ON currents were distributed within about 1 order of magnitude while the OFF currents seemed to be somewhat broader. The ON and OFF currents

were separated by 3 orders of magnitude, which is enough value for demonstrating reliable bistability of resistive memory devices. The distributions of threshold voltages of P**BAB**75 devices also showed the superb cell-to-cell uniformity. As the amount of **B** block decreased (from P**BAB**75 to -15), statistical performance data in terms of cumulative probability and distributions of threshold voltages became poor. The broadness of distribution of the ON currents became wider, and the average ON currents decreased in moving from P**BAB**75 to -15. Although the distribution of OFF currents was to some extent improved, ON/OFF ratios were decreased from P**BAB**75 to -15, degrading bistability of resistive memory devices. The declinable behavior of device uniformity was also observed in distributions of threshold voltages. The broadness and mean value of distributions of threshold voltages were increased from P**BAB**75 to -15.

As discussed in Figure 3, the P**BAB**75 showed well-ordered microphase-separated morphological structures in contrast with poorly ordered structures of P**BAB**45 and P**BAB**15. It has been
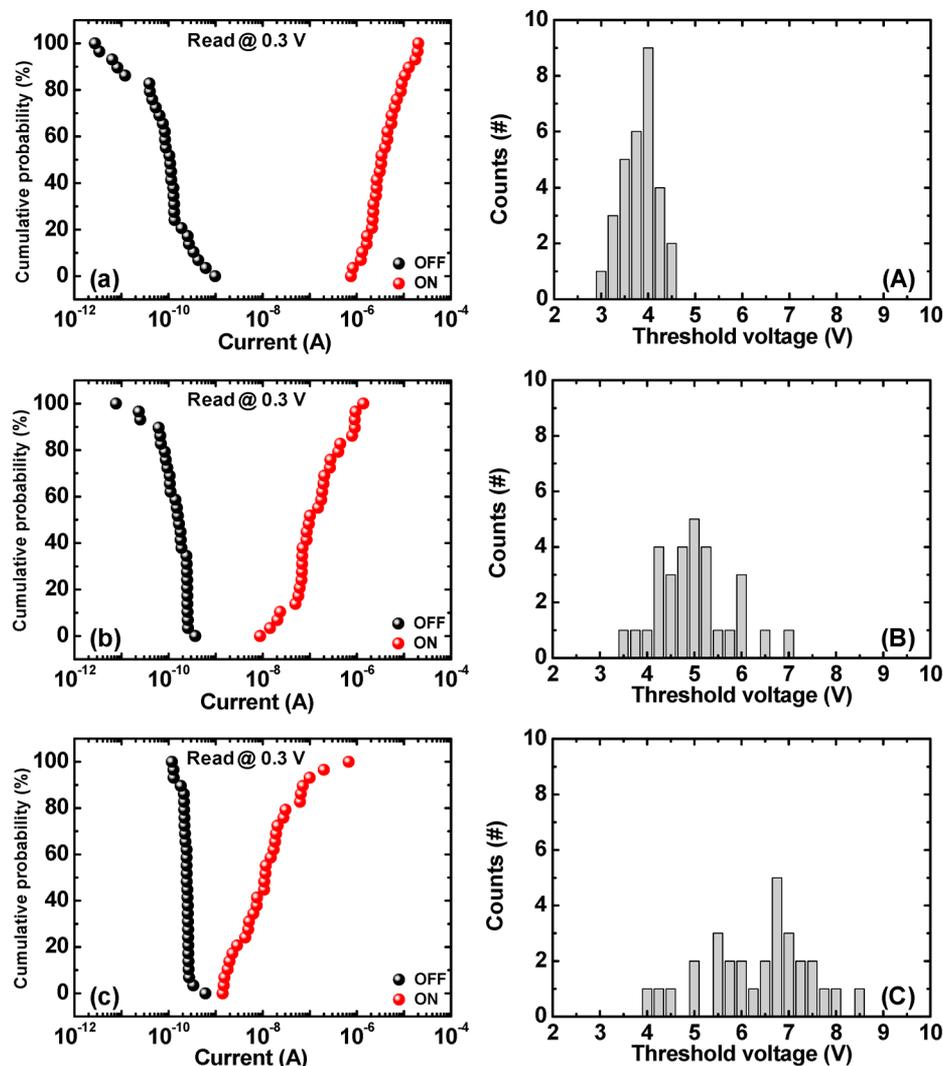
Figure 7. Cumulative probability of ON and OFF states and statistical distributions of the threshold voltages of (a, A) P**BAB**75, (b, B) P**BAB**45, and (c, C) P**BAB**15.

proved from the previous researches that the memory devices fabricated with block copolymer active layers showing well-ordered microphase-separated morphological structures exhibit excellent memory performances because the accessibility and reproducibility of filamentary conduction paths are especially outstanding in well-ordered film morphologies.[9,14] This suggests that filamentary paths are most favorably grown and then easily broke up in well-ordered microphase-separated structures of the block copolymers, resulting in nonvolatile resistive switching characteristics with high performances. For this reason, among three kinds of devices, P**BAB**75 probably leads to the lowest threshold voltages and the highest ON current values from bistable accessibility of filamentary conduction paths and the smallest broadness of distributions of threshold voltages from morphological stability of P**BAB**75 active layer in the devices.

Figure 8 shows the dc sweep endurance cycles and retention times of each P**BAB**-based memory device. The endurance cycling data were obtained from repetitive set and reset process in the $I-V$ sweep test of a single cell in each P**BAB** device. Even though all the devices showed ON/OFF ratios of approximately 10^4 in repetitive dc $I-V$ cycling test, the significant distinction of endurance reliability was observed as follows: 230, 140, and 90 cycles for P**BAB**75, P**BAB**45, and P**BAB**15, respectively. The devices with P**BAB**75 exhibited the most excellent electrical reproducibility as compared to that of both P**BAB**45 and P**BAB**15, indicating practical memory applicability of P**BAB**75. This result also might originate from well-ordered microphase-separated film morphologies of P**BAB**75 that stably experienced the repetitive formation and rupture of resistive semiconducting paths in the block copolymer. Figure 8d shows the retention characteristics of the ON and OFF states in each memory device at a read voltage of 0.3 V. Each bistable ON and OFF current was well maintained for a long retention time of 10^4 s in the P**BAB**75 and P**BAB**45 devices; however, there was serious degradation of ON current in process of time in the P**BAB**15 device, indicating that the P**BAB**75 can be the most suitable active layer for the application of polymer resistive memory device.

■ CONCLUSIONS

The well-defined block copolymers with triphenylamine group as a conducting moiety and isocyanate group as an insulating moiety were successfully synthesized without undesirable side reactions in the presence of NaBPh$_4$ for polymer memory applications. The precise synthesis of novel block copolymers is
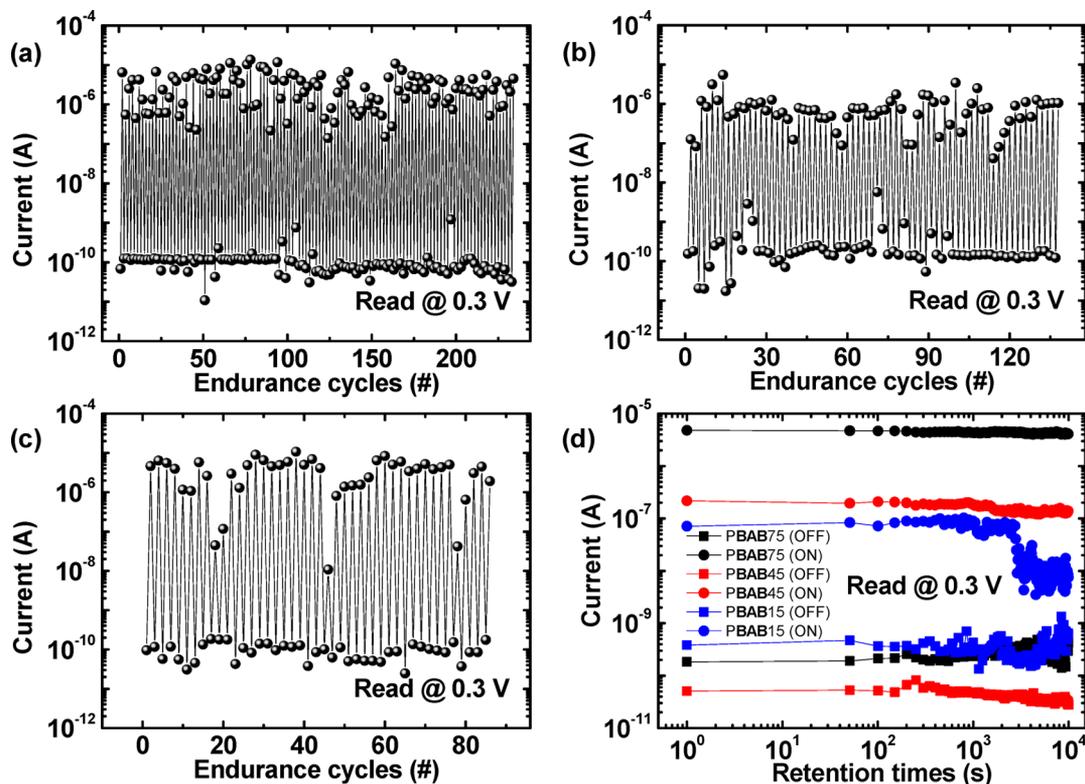
Figure 8. Dc sweep endurance characteristics of (a) PBAB75, (b) PBAB45, and (c) PBAB15. (d) Retention time of PBAB75, PBAB45, and PBAB15.

due to the addition of NaBPh$_4$, which can exchange countercation from K$^+$ to Na$^+$ for the living anionic polymerization of **B**. It was found that the morphological film structures of precisely controlled block copolymers (PBAB75, PBAB45, and PBAB15) were strongly dependent on block ratios. These morphological behaviors of the block copolymers significantly affected the performances of polymer resistive memory devices. All memory devices exhibited nonvolatile memory characteristics that are governed by the trap-controlled SCLC mechanism and filament formation. Among them, PBAB75-based devices with well-ordered microphase-separated film morphologies particularly showed excellent memory performances in terms of electrical properties, mechanical reliability, cell-to-cell uniformity, and practicability from the morphological superiority than PBAB45 and PBAB15.

■ ASSOCIATED CONTENT

Ⓢ Supporting Information

SEC curves of PBAB45 and PBAB15; the double-log $I–V$ plots of PBAB45 and PBAB15 memory devices. This material is available free of charge via the Internet at http://pubs.acs.org.

■ AUTHOR INFORMATION

Corresponding Authors

*Tel +82-62-715-2306; Fax +82-62-715-2304; e-mail jslee@gist.ac.kr (J.-S.L.).
*Tel +82-2-880-4269; Fax +82-2-884-3005; e-mail tlee@snu.ac.kr (T.L.).

Author Contributions

B.-G.K. and J.J. contributed equally to this work.

Notes

The authors declare no competing financial interest.

■ REFERENCES

(1) Park, J. H.; Yun, C.; Park, M. H.; Do, Y.; Yoo, S.; Lee, M. H. *Macromolecules* **2009**, *42*, 6840.
(2) Yeh, K.-M.; Lee, C.-C.; Chen, Y. *Synth. Met.* **2008**, *158*, 565.
(3) Mutaguchi, D.; Okumoto, K.; Ohsedo, Y.; Moriwaki, K.; Shirota, Y. *Org. Electron.* **2003**, *4*, 49.
(4) Feast, W. J.; Peace, R. J.; Sage, I. C.; Wood, E. L. *Polym. Bull.* **1999**, *42*, 167.
(5) Bellmann, E.; Shaheen, S. E.; Grubbs, R. H.; Marder, S. R.; Kippelen, B.; Peyghambarian, N. *Chem. Mater.* **1999**, *11*, 399.
(6) Kang, B.-G.; Kang, N.-G.; Lee, J.-S. *Macromolecules* **2010**, *43*, 8400.
(7) Higashihara, T.; Ueda, M. *Macromolecules* **2009**, *42*, 8794.
(8) Natori, I.; Natori, S.; Usui, H.; Sato, H. *Macromolecules* **2008**, *41*, 3852.
(9) Kang, B.-G.; Song, S.; Cho, B.; Kang, N.-G.; Kim, M.-J.; Lee, T.; Lee, J.-S. *J. Polym. Sci., Part A: Polym. Chem.* **2014**, *52*, 2625.
(10) Kang, B.-G.; Yu, Y.-G.; Kang, N.-G.; Lee, J.-S. *J. Polym. Sci., Part A: Polym. Chem.* **2013**, *51*, 4233.
(11) Kang, B.-G.; Kang, H.; Kang, N.-G.; Lee, C.-L.; Lee, K.; Lee, J.-S. *Polym. Chem.* **2013**, *4*, 969.
(12) Kim, K.; Kim, Y. Y.; Park, S.; Ko, Y.-G.; Rho, Y.; Kwon, W.; Shin, T. J.; Kim, J.; Ree, M. *Macromolecules* **2014**, *47*, 4397.
(13) Ahn, B.; Kim, D. M.; Hsu, J.-C.; Ko, Y.-G.; Shin, T. J.; Kim, J.; Chen, W.-C.; Ree, M. *ACS Macro Lett.* **2013**, *2*, 555.
(14) Kang, N.-G.; Cho, B.; Kang, B.-G.; Song, S.; Lee, T.; Lee, J.-S. *Adv. Mater.* **2012**, *24*, 385.

(15) Bolton, J. M.; Hillmyer, M. A.; Hoye, T. R. *ACS Macro Lett.* **2014**, *3*, 717.

(16) Tanaka, S.; Goseki, R.; Ishizone, T.; Hirao, A. *Macromolecules* **2014**, *47*, 2333.

(17) Kang, B.-G.; Kang, N.-G.; Lee, J.-S. *J. Polym. Sci., Part A: Polym. Chem.* **2011**, *49*, 5199.

(18) Hirao, A.; Matsuo, Y.; Oie, T.; Goseki, R.; Ishizone, T.; Sugiyama, K.; Gröschel, A. H.; Müller, A. H. E. *Macromolecules* **2011**, *44*, 6345.

(19) Tsoukatos, T.; Avgeropoulos, A.; Hadjichristidis, N.; Hong, K.; Mays, J. W. *Macromolecules* **2002**, *35*, 7928.

(20) Ahn, J.-H.; Lee, J.-S. *Macromol. Rapid Commun.* **2003**, *24*, 571.

(21) Shin, Y.-D.; Han, S.-H.; Samal, S.; Lee, J.-S. *J. Polym. Sci., Part A: Polym. Chem.* **2005**, *43*, 607.

(22) Tsuda, K.; Ishizone, T.; Hirao, A.; Nakahama, S.; Kakuchi, T.; Yokota, K. *Macromolecules* **1993**, *26*, 6985.

(23) Cho, B.; Kim, T.-W.; Choe, M.; Wang, G.; Song, S.; Lee, T. *Org. Electron.* **2009**, *10*, 473.

(24) Kim, T.-W.; Zeigler, D. F.; Acton, O.; Yip, H.-L.; Ma, H.; Jen, A. K.-Y. *Adv. Mater.* **2012**, *24*, 828.

(25) Arif, M.; Yun, M.; Gangopadhyay, S.; Ghosh, K.; Fadiga, L.; Galbrecht, F.; Scherf, U.; Guha, S. *Phys. Rev. B* **2007**, *75*, 195202.

(26) Kim, T.-W.; Oh, S.-H.; Choi, H.; Wang, G.; Hwang, H.; Kim, D.-Y.; Lee, T. *Appl. Phys. Lett.* **2008**, *92*, 253308.

(27) Jo, H.; Ko, J.; Lim, J. A.; Chang, H. J.; Kim, Y. S. *Macromol. Rapid Commun.* **2013**, *34*, 355.

(28) Ji, Y.; Choe, M.; Cho, B.; Song, S.; Yoon, J.; Ko, H. C.; Lee, T. *Nanotechnology* **2012**, *23*, 105202.

(29) Liu, J.; Yin, Z.; Cao, X.; Zhao, F.; Lin, A.; Xie, L.; Fan, Q.; Boey, F.; Zhang, H.; Huang, W. *ACS Nano* **2010**, *4*, 3987.

(30) Wang, Z. S.; Zeng, F.; Yang, J.; Chen, C.; Yang, Y. C.; Pan, F. *Appl. Phys. Lett.* **2010**, *97*, 253301.

(31) Lin, W.-P.; Liu, S.-J.; Gong, T.; Zhao, Q.; Huang, W. *Adv. Mater.* **2014**, *26*, 570.